SANDIA REPORT SAND81-1390 • Unlimited Release
Printed December 1981

# LOVEL:
# A Low-Velocity Aerodynamic Heating Code for Flat-Plates, Wedges, and Cones



Anthony L. Thornton



Prepared by
Sandia National Laboratories
Albuquerque, New Mexico 87185 and Livermore, California 94550
for the United States Department of Energy
under Contract DE-AC04-76DP00789

## DISCLAIMER

Issued by Sandia National Laboratories, operated for the United States Department of Energy by Sandia Corporation.



Printed in the United States of America
Available from
National Technical Information Service
U.S. Department of Commerce
5285 Port Royal Road
Springfield, VA 22161

NTIS price codes
Printed copy: $6.00
Microfiche copy: A01

PAGES 1 to 2

WERE INTENTIONALLY

LEFT BLANK

SAND81-1390
Unlimited Release
Printed December 1981

SAND--81-1390

DE82 007100

# LOVEL: A Low-Velocity Aerodynamic Heating Code for Flat-Plates, Wedges, and Cones

Anthony L. Thornton
Aerothermodynamics Division 5633
Sandia National Laboratories
Albuquerque, NM 87185

## Abstract

The LOVEL computer program calculates the boundary-layer edge conditions for subsonic and supersonic flow over flat-plate, wedge, and cone geometries for freestream Mach conditions ($M_\infty$) < 3. Cold-wall heat-transfer calculations use reference temperature correlations based on boundary-layer edge Mach number to compute fluid properties. The first part of this report describes the theory used in the computation of the cold-wall heat-transfer rates; the second part describes in detail the input/output format for the LOVEL computer program. Outputs include freestream conditions, boundary-layer edge conditions, cold-wall heat-transfer rates, plots of heating rates, and punched-card output for use in ablation and in-depth transient heat-conduction computer codes.

## Acknowledgments

The author acknowledges the contributions of S. G. Beard and S. McAlees for their guidance and instruction in the editing of this report. Also, the author thanks R. Palmer for furnishing the plot subroutine and D. E. Larson for his computational assistance with the program.

# Contents



# Illustrations

**Figure**

## Symbols

| | |
|---|---|
| $a$ | Speed of sound (ft/sec) |
| $C_f$ | Skin friction coefficient |
| $H_{cw}$ | Cold-wall enthalpy (Btu/lbm) |
| $H_r$ | Recovery enthalpy (Btu/lbm) |
| $h_s$ | Local heat-transfer coefficient (Btu/ft$^2$-sec-°R) |
| JANAF | Joint Army-Navy-Air Force thermochemical data system |
| K | Hypersonic similarity parameter |
| k | Thermal conductivity (Btu/ft-sec-°R) |
| M | Mach number |
| P | Pressure (atm) |
| Pr | Prandtl number |
| $\dot{q}$ | Heat transfer rate per unit area (Btu/ft$^2$-sec) |
| Re | Reynolds number |
| St | Stanton number |
| T | Temperature (°R) |
| U | Velocity (ft/sec) |

## Greek

| | |
|---|---|
| $\beta$ | Included wedge angle factor |
| $\gamma$ | Ratio of specific heats, $\gamma = 1.4$ |
| $\delta$ | Wedge or cone half-angle (deg) |
| $\theta_s$ | Wedge or cone shock angle (deg) |
| $\mu$ | Viscosity (lbm/ft-sec) |
| $\Delta$ | Momentum thickness (ft) |

## Subscripts

| | |
|---|---|
| C | Cone value |
| cw | Cold-wall value referenced to 536 °R |
| e | Boundary layer outer edge conditions |
| f | Flat-plate value |
| LAM | Laminar Flow |
| o | Initial estimate |
| s | Arc location |
| TURB | Turbulent flow |
| w | Conditions at the wall |
| wg | Wedge value |
| x | Axial location |
| 1N | Conditions normal to and in front of shock |
| 2N | Conditions normal to and behind shock |
| $\infty$ | Freestream conditions |

## Superscripts

| | |
|---|---|
| o | Corresponding incompressible value |
| * | Eckert's reference conditions |

# LOVEL: A Low-Velocity Aerodynamic Heating Code for Flat-Plates, Wedges, and Cones

## Part I: Theory

### Introduction

Computer programs to predict aerodynamic heating on reentry vehicles and rockets at $M_\infty > 2.0$ and altitudes less than 200 kft have been used at Sandia National Laboratories in Albuquerque (SNLA) for several years. Recently, however, there have been numerous projects, such as reentry vehicle recovery via parachute deployment, in which the aerodynamic bodies experienced low-velocity heating or cooling for relatively long periods of time. Previous heating analyses of these bodies at $M_\infty < 2.0$ involved the use of simplified hand calculations of the relevant heat-transfer equations over a flat-plate.

The LOVEL program was written to obtain more accurate predictions of aerodynamic heating for flat-plates, wedges, and cones at $M_\infty < 3.0$. This program computes boundary-layer edge conditions, assuming a perfect gas, and cold-wall heat transfer rates based on a reference temperature. In addition to computing the cold-wall heat-transfer rates, program output includes the freestream conditions, plots of heating rates, and punched card output for use in ablation and in-depth transient heat conduction computer codes.

The following presentation describes the theory used in the computational procedure, the program input format, and the various output options available to the user. A listing of an input card deck and an example of printed output are also presented. A graph indicating the minimum supersonic Mach numbers as a function of wedge or cone angle, for which the governing equations are applicable, is included in Appendix A.

### Discussion of Program Theory

#### Subsonic Flow

To determine the local velocity profile over a flat-plate or wedge in incompressible flow, one may use the Falkner-Skan solution

$$U_e(s) = U_\infty s^m \tag{1}$$

where the exponent, m, is determined from the relation

$$m = \frac{\beta}{2 - \beta} \tag{2}$$

and $\beta$ represents the included wedge angle factor (Figure 1) through which the inviscid flow is turned. $\beta$ may be defined by the wedge semivertex angle, $\delta_w$, using the expression

$$\beta = \frac{\delta_w}{90} \tag{3}$$

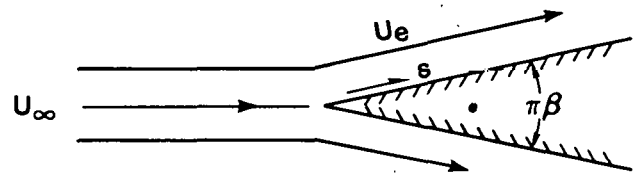


**Figure 1.** Streamlines for Potential Flow Described by Equation (1)

For conical flow, potential theory states that

$$U_e(s) = U_\infty s^n \tag{4}$$

where $U_e$ represents the inviscid velocity at the surface of a cone with semivertex angle, $\delta_c$, at zero angle of attack. The relationship between the exponent n and the semivertex angle, $\delta_c$, is not as simple as the Falkner-Skan wedge flow relationship defined by Eq (2). Tabulated values of n as a function of $\delta_c$ are given in Ref 1. For the small cone angles associated with reentry vehicles ($0° \leq \delta_c \leq 15°$), n can be approximated by the linear expression

$$n = 2.68 \cdot \delta_c \times 10^{-3} \tag{5}$$

where $\delta_c$ is in degrees. Note that for the angles of interest, n is very small. Consequently, local conditions are very nearly equal to freestream conditions. For further discussion on the potential flow past a cone of semivertex angle $\delta_c$, consult Ref 2.

After determining the local velocity, the local enthalpy is calculated by using the expression

$$H_e = H_\infty + \frac{1}{50{,}073}\left(U_\infty^2 - U_e^2\right) . \tag{6}$$

Similarly, the local temperature, pressure, and density can be determined from

$$\frac{T_e}{T_\infty} = 1 - \frac{\gamma - 1}{2} M_\infty^2 \left[\left(\frac{U_e}{U_\infty}\right)^2 - 1\right] \tag{7}$$

$$\frac{P_e}{P_\infty} = \left\{1 - \frac{\gamma - 1}{2} M_\infty^2 \left[\left(\frac{U_e}{U_\infty}\right)^2 - 1\right]\right\}^{\frac{\gamma}{\gamma-1}} = \left(\frac{T_e}{T_\infty}\right)^{\frac{\gamma}{\gamma-1}} \tag{8}$$

$$\frac{\rho_e}{\rho_\infty} = \left\{1 - \frac{\gamma - 1}{2} M_\infty^2 \left[\left(\frac{U_e}{U_\infty}\right)^2 - 1\right]\right\}^{\frac{1}{\gamma-1}} = \left(\frac{T_e}{T_\infty}\right)^{\frac{1}{\gamma-1}} . \tag{9}$$

The local viscosity of air, as determined from the Sutherland equation, is given as

$$\mu_e = 7.30395 \frac{(T_e)^{3/2}}{T_e + 198.6} \times 10^{-7} \tag{10}$$

whereby the local Reynolds number may be calculated from the expression

$$Re_s = \frac{\rho_e U_e s}{\mu_e} . \tag{11}$$

Once the edge conditions have been properly evaluated, the local heat-transfer rate can be computed. It is important to note that at the moderate flight velocities considered in this analysis, aerodynamic heating is low. Yet, temperature gradients do exist across the boundary layer and as a result, significant density changes may also occur across the boundary layer. The assumption of an incompressible boundary layer is less valid for moderate velocities ($M_\infty < 3.0$) than it is for high velocities. The reason is that at hypersonic velocities, higher temperatures exist, yet lower gradients appear within the boundary layer; hence, the gas becomes "stiffer" and acts more like an incompressible fluid. As a result, to obtain engineering accuracy in the heat-transfer calculations, all fluid properties were evaluated at a reference temperature.

For a laminar boundary layer, the recovery enthalpy is defined as

$$H_r = H_e + (Pr^*)^{1/2} \frac{U_e^2}{50{,}073} \tag{12}$$

and for a turbulent boundary layer

$$H_r = H_e + (Pr^*)^{1/3} \frac{U_e^2}{50{,}073} \tag{13}$$

where $Pr^* = \mu^* C_p^*/k^*$. Appendix B describes the transition criterion used in this analysis. Using the empirical correlation of Eckert,[1] the reference temperature for laminar flow is given by

$$\frac{T^*}{T_e} = 0.5 + 0.39 M_e^2 + 0.5 \frac{T_w}{T_e} \tag{14}$$

and the corresponding expression for turbulent flow[1] is

$$\frac{T^*}{T_e} = 0.5 + 0.023 M_e^2 + 0.5 \frac{T_w}{T_e} . \tag{15}$$

Table 1 gives the specific heat and thermal conductivity as a function of temperature.[4] These parameters can be used to compute the value of the reference Prandtl number.

**Table 1. Properties of Dry Air at Atmospheric Pressure**

| Temperature (°R) | Specific Heat* (ft-lb/slug-°R) | Thermal Conductivity** (ft-lb/ft-hr-°R) |
|---|---|---|
| 450 | 6012.3 | 10.013 |
| 522 | 6015.7 | 11.45 |
| 540 | 6017.8 | 11.80 |
| 576 | 6023.3 | 12.49 |
| 612 | 6030.7 | 13.17 |
| 648 | 6039.9 | 13.84 |
| 684 | 6051.5 | 14.49 |
| 720 | 6064.8 | 15.13 |
| 774 | 6088.5 | 16.08 |
| 810 | 6106.7 | 16.68 |
| 846 | 6126.6 | 17.29 |
| 882 | 6147.9 | 17.88 |
| 900 | 6159.1 | 18.17 |
| 936 | 6182.6 | 18.75 |
| 990 | 6220.2 | 19.59 |

*Multiply tabulated values of $C_p$ by $3.9942 \times 10^{-5}$ to obtain Btu/lbm-°R.

**Multiply tabulated values of k by $3.5697 \times 10^{-7}$ to obtain Btu/ft-sec-°R.

To deduce the cold-wall heat-transfer characteristics, flat-plate theory will be imposed. According to Ref 5, the heat flow at the wall is given by

$$\dot{q} = \frac{h_s}{C_p^*} (H_r - H_w) \tag{16}$$

where $h_s$ represents the local heat-transfer coefficient at station s. Employing the definition of Stanton number,

$$St_s^* = \frac{h_s}{\rho^* U_e C_p^*} , \tag{17}$$

where

$$\rho^* = \rho_e \left(\frac{T_e}{T^*}\right) , \tag{18}$$

experimental research indicates that

$$St_s^* = \frac{C_f}{2} (Pr^*)^{-2/3} . \tag{19}$$

The skin friction coefficient in Eq (19) for incompressible laminar flow is expressible as

$$C_f^\circ)_{LAM} = 0.664 (Re_s^*)^{-1/2} . \tag{20}$$

Similarly for turbulent flow, the applicable skin friction coefficient relationship is

$$C_f^\circ)_{TURB} = 0.0578 (Re_s^*)^{-1/5} . \tag{21}$$

After some simple substitutions, the laminar and turbulent Stanton numbers can be shown to equal

$$St_s^*)_{LAM} = 0.332 (Pr^*)^{-2/3} (Re_s^*)^{-1/2} \tag{22}$$

and

$$St_s^*)_{TURB} = 0.0289 (Re_s^*)^{-1/5} (Pr^*)^{-2/3} . \tag{23}$$

From Eq (17), it follows that

$$h_s = \rho^* U_e C_p^* St_s^*$$

from which Eq (16) can be rewritten as

$$\dot{q}_{cw} = \rho^* U_e St_s^* (H_r - H_w) , \tag{24}$$

where the expression given by Eq (24) is applicable for either laminar or turbulent flow, the only difference being in the defining equations for $St_s^*$ and $H_r$. Eq (24) can be rearranged so that

$$\dot{q}_{cw} = \frac{\rho^* U_e S}{\mu^*} St_s^* (H_r - H_w) \frac{\mu^*}{\varepsilon} ; \tag{25}$$

hence, for laminar flow, the heat transfer rate per unit area is

$$\dot{q}_{cw})_{LAM} = 0.332 (Re_s^*)^{1/2} (Pr^*)^{-2/3} (H_r - H_w) \frac{\mu^*}{s} \tag{26}$$

and for turbulent flow

$$\dot{q}_{cw})_{TURB} = 0.0289 (Re_s^*)^{0.8} (Pr^*)^{-2/3} (H_r - H_w) \frac{\mu^*}{s} . \tag{27}$$

Note that Eqs (26) and (27) apply for flow over a flat-plate or wedge. For conical flow, it can be shown by use of Mangler's transformation that the local cone skin-friction coefficient is related to the flat-plate skin-friction coefficient by the relation

$$C_{f_{LAM}})_c = \sqrt{3}\ C_{f_{LAM}})_f \quad (28)$$

if the local Reynolds numbers are equal. Note that Eq (28) is applicable only for laminar flow over the cone. For turbulent flow over the cone, the skin friction coefficients are related by

$$C_{f_{TURB}})_c = 1.17\ C_{f_{TURB}})_f \quad . \quad (29)$$

Consequently, in order to determine the heat transfer rate over the surface of a cone, Eq (26) should be multiplied by the factor $\sqrt{3}$, if the flow is laminar, or Eq (27) should be multiplied by the factor 1.17 for turbulent flow. Note that this should be done for both subsonic and supersonic flight regimes.

## Supersonic Flow

For supersonic flow in the range $3 > M_\infty > 1$, the following procedure was used to determine the conditions behind the shock of a sharp cone, wedge, or flat-plate at zero angle of attack. It is important to realize that before the boundary-layer edge conditions are calculated, the shock angle, $\theta_s$, must be determined. Over a flat-plate, the shock angle is equal to the Mach Line, which is given by

$$\theta_{s_f} = \sin^{-1}\frac{1}{M_\infty} \quad . \quad (30)$$

In the case of wedge flow in a perfect gas, the relationship between the deflection angle and the shock angle is described by

$$\cot(\delta_{wg}) = \tan(\theta_s)\left[\frac{(\gamma+1)M_\infty^2}{2(M_\infty^2\sin^2\theta_s - 1)} - 1\right]$$

$$= \tan(\theta_s)\left[\frac{6\,M_\infty^2}{5(M_\infty^2\sin^2\theta_s - 1)} - 1\right] \quad (31)$$

where $\delta_{wg}$ is known and $\gamma = 1.4$. To determine the correct shock angle, Eq (31) is iterated upon until

$$(\theta_s^{n+1} - \theta_s^n) \leq \epsilon \quad , \quad (32)$$

where the superscripts refer to the n+1 and the $n^{th}$ iterative value of the shock angle, and $\epsilon$ refers to some error criteria (usually less than $10^{-3}$). For rapid convergence, a Newton-Raphson iterative scheme was applied to Eq (31). Appendix C outlines the procedure used in the convergence scheme.

The dependence of shock wave angle on cone semivertex angle at various freestream Mach numbers is given for conical flow in Ref 6. It is apparent for low Mach numbers and for cone semivertex angles less than 7° that the shock-wave angle is nearly independent of the semivertex angle. Reference 5 uses a hypersonic similarity parameter to give an equation for the shock angle as a function of freestream Mach number and cone angle. This equation is given by

$$M_\infty \sin\theta_s = \left(1 + \frac{\gamma+1}{2}K_1^2\right)^{1/2} \quad , \quad (33)$$

where $K_1$ represents the aforementioned hypersonic similarity parameter defined as

$$K_1 = M_\infty \sin(\delta_c) \quad . \quad (34)$$

Note that in the use of the similarity parameter, there is no restriction on the cone angle or freestream Mach number except that

$$K_1 \leq 6$$

and

$$M_\infty > 1.0. \quad (35)$$

For wedges or flat-plates, once the shock angle, $\theta_s$, is computed, determination of the normal Mach numbers ahead of and behind the shock are easily calculated by using the following relations

$$M_{1N} = M_\infty \sin\theta_s \quad (36)$$

and

$$M_{2N}^2 = \frac{(\gamma-1)M_{1N}^2 + 2}{2\gamma M_{1N}^2 - (\gamma-1)} = \frac{M_{1N}^2 + 5}{7M_{1N}^2 - 1} \quad (37)$$

from which the local conditions behind the shock are given by

$$\frac{P_e}{P_\infty} = \frac{2\gamma M_{1N}^2 - (\gamma-1)}{\gamma+1} = \frac{7M_{1N}^2 - 1}{6} \quad (38)$$

$$\frac{\rho_e}{\rho_\infty} = \frac{(\gamma+1)M_{1N}^2}{(\gamma-1)M_{1N}^2 + 2} = \frac{6M_{1N}^2}{M_{1N}^2 + 5} \quad (39)$$

$$\frac{T_e}{T_\infty} = \frac{P_e\,\rho_\infty}{P_\infty\,\rho_e} = \frac{(7M_{1N}^2 - 1)\ (M_{1N}^2 + 5)}{36M_{1N}^2} \quad . \quad (40)$$

Recalling that

$$a_e = \sqrt{\gamma R T_e} \cong 49.02 \sqrt{T_e} \tag{41}$$

where the velocity of sound is in units of feet per second and $T_e$ is in degrees Rankine, the normal velocity behind the shock is given by

$$U_{2N} = M_{2N} \cdot a_e \tag{42}$$

and the tangential velocity is

$$U_{2T} = a_\infty M_\infty \cos \theta_s = U_\infty \cos \theta_s \, . \tag{43}$$

Consequently, the total velocity is expressible as

$$U_e = \sqrt{U_{2N}^2 + U_{2T}^2} \, . \tag{44}$$

The local enthalpy can now be determined from

$$H_e + H_\infty + \frac{1}{2} (U_\infty^2 - U_e^2) \tag{45}$$

where it folllows that the recovery enthalpy is given by Eq (12) or (13), depending upon whether or not the flow is laminar or turbulent.

Note that Eqs (38), (39), and (40) are applicable for flat-plate or wedge flow only. In the case of conical flow, the pressure and enthalpy on the cone surface can be approximated by

$$\left(\frac{P_e}{P_\infty}\right)_c = 1.993 \, (K_1)^{1.98} + 1.302 \tag{46}$$

$$\left(\frac{H_e}{H_\infty}\right)_c = 0.240 \, (K_1)^{1.97} + 1.119 \tag{47}$$

and the surface velocity can then be calculated from

$$\left(\frac{U_e}{U_\infty}\right)^2 = \frac{2}{(\gamma - 1) M_\infty^2} \left(1 + \frac{\gamma - 1}{2} M_\infty^2 - \frac{H_e}{H_\infty}\right)$$

$$= \frac{5}{M_\infty^2} \left(1 + \frac{M_\infty^2}{5} - \frac{H_e}{H_\infty}\right) \tag{48}$$

for $\gamma = 1.4$.

The cone edge temperature is determined from an iteration of the following

$$T_e^{n+1})_c \approx H_e / C_p \, (T_e^n) \tag{49}$$

and the edge density is given by

$$\left(\frac{\rho_e}{\rho_\infty}\right)_c = \left(\frac{P_e}{P_\infty}\right)_c \cdot \left(\frac{T_\infty}{T_e}\right)_c \tag{50}$$

Finally, the cone edge Mach number is computed from

$$M_c = \frac{U_e}{a_e} = \frac{U_e}{49.02} \, (T_e)^{-1/2} \, , \tag{51}$$

and all of the local properties have now been evaluated. Depending upon whether the flow is laminar or turbulent, a reference temperature is calculated through the use of Eq (14) or (15). As a result, $\mu^*$, $Pr^*$, $Re^*$, $C_p^*$, and all other temperature dependent quantities can be determined. Note that Eqs (26) and (27) for the heat-transfer rate are just as applicable for supersonic flow as they were for subsonic flow.

# Application

The evaluation of a computer program requires that the results obtained compare favorably to existing computer codes which were developed for the same or similar purposes. In all cases, the computer program must accurately predict the physical phenomena it was intended to model. Consequently, verification of computer predictions through experimental data is expected whenever possible.

Investigation of the LOVEL code for accuracy involved two distinct phases. The first phase involved a comparison between LOVEL and BLUNTY,[7] using the same vehicle trajectory. The second phase involved comparing LOVEL with actual flight test results. To accomplish both objectives, data were obtained from a previously flown test trajectory of a Standard missile. Particular interest was given to two stations on the cylindrical portion of the vehicle far enough away from the nosetip to eliminate bluntness effects. For the test trajectory flown, freestream Mach numbers ranged from 0.0 to 5.0; and although LOVEL was intended for $M_\infty < 3.0$, the Mach numbers were considered low enough for the purpose of this comparison.

Program BLUNTY, currently used at Sandia National Laboratories, is a procedure developed for computing aerodynamic heating on sphere cones at zero angle of attack. BLUNTY calculations have been compared with actual flight data and show excellent agreement for $M_\infty > 2.0$. For this comparative analysis, the flat-plate option of the LOVEL heating code

was chosen to calculate the boundary-layer edge conditions. Figures 2 and 3 show the difference between heating rate, edge pressure, recovery enthalpy, and heat transfer coefficient as predicted by LOVEL and BLUNTY for two different arc locations. Notice that LOVEL closely approaches the values predicted by BLUNTY for the quantities considered. Predicted heating rates differ by less then 6.0% at the front station for the entire trajectory and show a maximum difference of 17.0% at the aft station. These differences are due, in part, to the fact that BLUNTY accounts for real gas effects (e.g., dissociation and changes in entropy through the shock), whereas LOVEL does not. Finally, Figure 4 shows the predictive capabilities of both programs when compared to preliminary flight test data for the peak heating portion of the trajectory. Execution time for running BLUNTY was approximately 250 sec as compared to 25 sec for LOVEL. It is evident that the LOVEL aerodynamic heating code should significantly improve current prediction capabilities in the low-velocity flight regime.

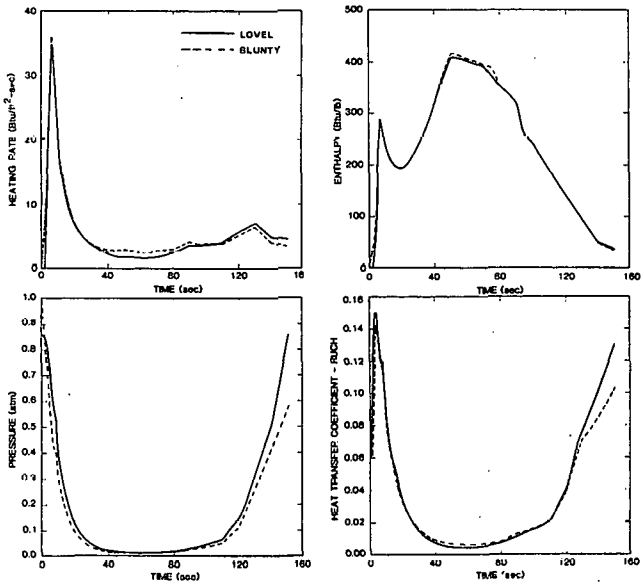


**Figure 2.** Heating Rate, Edge Pressure, Recovery Enthalpy, and Heat Transfer Coefficient Comparison of LOVEL and BLUNTY at the 37.1-In. Station

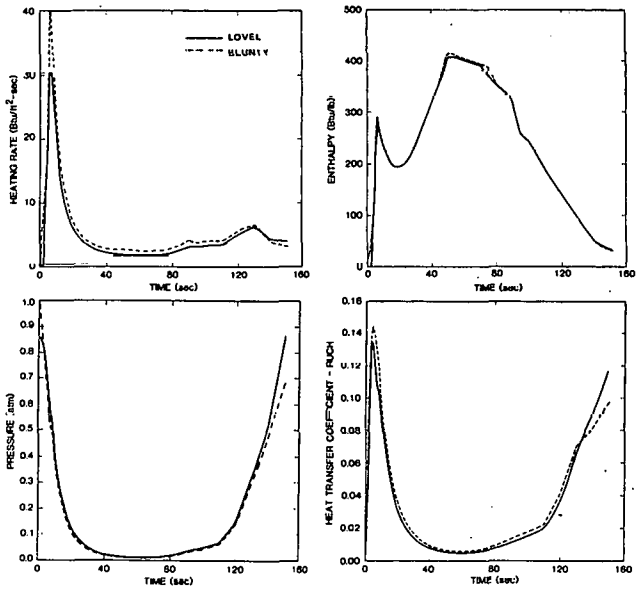


**Figure 3.** Heating Rate, Edge Pressure, Recovery Enthalpy, and Heat Transfer Coefficient Comparison of LOVEL and BLUNTY at the 66.6-In. Station

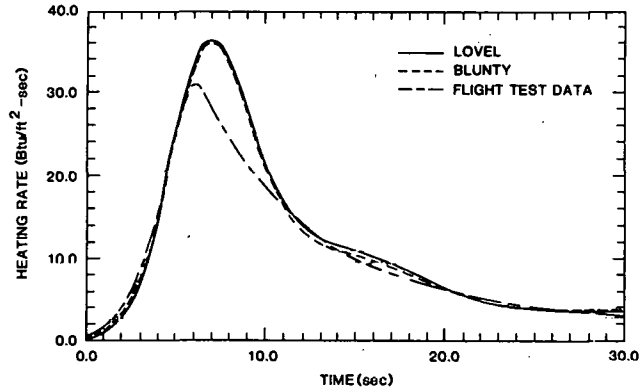


**Figure 4.** Heating Rate Comparison Between LOVEL, BLUNTY, and Flight Test Data

To ascertain the effects of vehicle geometry on the heating rate, separate runs were completed using the flat-plate, wedge, and cone geometry options available to the user. A 10-deg half-angle was used for the wedge and cone geometries. Figure 5 shows the results of the study. Given the same flight conditions and arc location, calculations indicate similar heat transfer rates for the wedge and cone geometries. This result occurs even though boundary-layer edge conditions differ. As expected, flat-plate heat transfer rates are considerably less than the corresponding wedge and conical flow values.

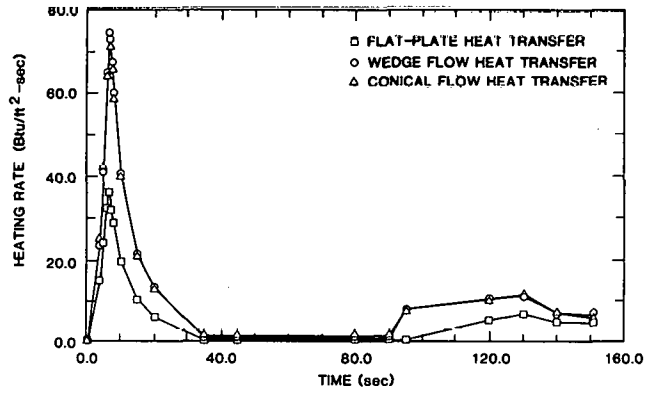


**Figure 5.** Effects of Vehicle Geometry on Heat Transfer Rate

## Conclusion

Using reference temperature correlations based on boundary-layer edge Mach number to compute fluid properties, the LOVEL aerodynamic heating code predicts coldwall heat transfer rates for flat-plate, wedge, and cone geometries. A comparison between BLUNTY and LOVEL indicates that the latter accurately predicts coldwall heat transfer rates on a vehicle surface which is far removed from the nosetip, thus eliminating the effects of bluntness (e.g., on the conical portion of a reentry vehicle). For the particular test cases run, it was discovered that LOVEL reduced the computational time by a factor of 10 as opposed to BLUNTY for predicting boundary layer edge conditions and heat transfer rates. Finally, the results of the present analysis reveal that LOVEL compares favorably with preliminary flight test heat transfer data.

# Part II: A User's Manual for the LOVEL Program

This part of the report summarizes the input requirements of the LOVEL program, provides specific instructions for program operation, and provides an explanation of the output.

## Program Input

The input to the LOVEL program has seven card sets. Five of the card sets must be present for each run to execute properly. The sixth card set of the program is required if the user wishes to input his own transition time. The seventh card set is required if plots are desired and the user wishes to input his own limits.

### Card Set 1 - Problem Identification and Page Heading

The user must supply three title cards. All 80 columns of the first two cards, and the first 10 columns of the third card are used to title the first page of output. The information in columns 1 through 10 on the third card is used to title subsequent output pages. Any alphanumeric information may be input.

**Cards 1-3**

| Card Cols | Format | Fortran Symbol | Description |
|---|---|---|---|
| 1-8 | 8A10 | TITLE1 | Problem identification |
| 1-80 | 8A10 | TITLE2 | Problem identification |
| 1-80 | A10 | VCN | Title |

### Card Set 2 - Body Geometry and Transition Criteria

The first card is required to input certain general parameters concerning the body geometry and to flag optional extras.

**Card 1**

| Card Cols | Format | Fortran Symbol | Description |
|---|---|---|---|
| 1-5 | I5 | N = 0 | Flat-plate |
| | | = 1 | Wedge |
| | | = 2 | Sharp cone |
| | | = 3 | Sphere cone (not currently used) |

**Card 1 (cont)**

| Card Cols | Format | Fortran Symbol | Description |
|---|---|---|---|
| 6-15 | E10.4 | DEL = 0.0 | Flat-plate |
| | | = $\delta_w$ | Wedge half-angle |
| | | = $\delta_c$ | Cone semivertex angle (deg.) |
| 16-20 | I5 | NTAU $\geq$ 1 | Number of times in trajectory $\leq$ 30 |
| 21-25 | I5 | IGEO $\geq$ 1 | Number of stations along body $\leq$ 15 |
| 26-30 | I5 | NSX = 0 | Stations are axial locations |
| | | = 1 | Stations are arc locations |
| 31-35 | I5 | | Transition criteria based on: |
| | | ITRAN = 0 | $Re_{,s}$ |
| | | = 1 | $Re_{,\theta}$ (not currently used) |
| | | = 2 | Time |
| 36-40 | I5 | | Do you wish to input your own transition criterion |
| | | IFLG1 = 0 | No |
| | | = 1 | Yes |
| 41-50 | E10.4 | TRNSTN < 0.0 | Flow initially turbulent and becomes laminar at Re = \|TRNSTN\| |
| | | = 0.0 | Flow remains turbulent throughout trajectory |
| | | > 0.0 | Flow initially laminar and becomes turbulent at Re = TRNSTN |
| | | = 9.9E + 15 | Flow remains laminar throughout trajectory |
| 51-60 | E10.4 | RN | Sphere cone nose radius (in.) (used only when N = 3) |

### Card Set 3 - Output Format

This card set designates the printout options for output and requests plots of heating rates.

| Card Cols | Format | Fortran Symbol | Description |
|---|---|---|---|
| 1-5 | I5 | IFLG6 = 0 | For each station, print edge conditions for entire trajectory |
| | | = 1 | For each time in the trajectory, print edge conditions for all stations |
| 6-10 | | | Do you want plots? |
| | I5 | IFLG7 = 0 | No |
| | | = 1 | Yes |

(cont)

| Card Cols | Format | Fortran Symbol | Description |
|---|---|---|---|
| 11-15 | I5 | | Do you want punched card output? |
| | | IFLG8 = 0 | No |
| | | = 1 | Yes |
| 16-20 | I5 | NPLOT | Number of card pairs in card 7. Applicable only when IFLG7 = 1. Either a single curve or multiple curves can be plotted on the same plot page. See card set 7 for explanation of plotting specifications. |

## Card Set 4 - Boundary Layer Edge and Freestream Conditions

Program LOVEL reads two cards for each time in the trajectory. The first card of this set contains the boundary-layer edge conditions and is ignored. The second card contains the freestream conditions. These cards can be obtained from the BLUNTY program. A maximum of 30 times is allowed in this set.

### Card 1 - Boundary-Layer Edge Conditions

| Card Cols | Format | Fortran Symbol | Description | Units |
|---|---|---|---|---|
| 1-2 | A2 | I2 | I2 = -1 on last card of set | |
| 3-10 | F8.3 | TIME | Time | sec |
| 11-20 | E10.4 | HR | Recovery enthalpy (JANAF) | Btu/lbm |
| 21-30 | E10.4 | TE | Edge temperature | °R |
| 31-40 | E10.4 | PE | Edge pressure | psia |
| 41-50 | E10.4 | RHOE | Edge density | $lbm/ft^3$ |
| 51-60 | E10.4 | UE | Edge velocity | ft/sec |
| 61-70 | E10.4 | ME | Edge Mach number | |
| 71-79 | A9 | ITIL | BLUNTY title | |
| 80 | A1 | ICON = L | Laminar flow | |
| | | = T | Turbulent flow | |

### Card 2 - Freestream Conditions

| Card Cols | Format | Fortran Symbol | Description | Units |
|---|---|---|---|---|
| 1-10 | F10.4 | TIME | Time | (sec) |
| 11-20 | F10.2 | U8 | Freestream velocity | (ft/sec) |
| 21-30 | F10.5 | T8 | Freestream temperature | (°R) |
| 31-40 | E10.4 | P8 | Freestream pressure | (psia) |
| 41-50 | E10.4 | RHO8 | Freestream density | $(lbm/ft^3)$ |
| 51-60 | F10.2 | H8 | Freestream enthalpy | (Btu/lbm) |
| 61-70 | E10.4 | MU8 | Freestream viscosity | (lbm/ft-sec) |
| 71-80 | F10.6 | M8 | Freestream Mach number | |

## Card Set 5 - Heating Locations

Heating locations are either axial (NSX = 0) or arc (NSX = 1) distances. A maximum of 15 station locations are allowed in this set.

| Card Cols | Format | Fortran Symbol | Description | Units |
|---|---|---|---|---|
| 1-80 | 8F10.5 | X or S | Heating locations | (in.) |

## Card Set 6 - Time of Transition and Relaminarization

This card should be used only when ITRAN = 2. When this option is chosen, the user should input a transition or relaminarization time.

| Card Cols | Format | Fortran Symbol | Description | Units |
|---|---|---|---|---|
| 1-10 | F10.5 | TRNTIM | Time of transition or relaminarization | (sec) |

## Card Set 7 - Plot Limits Card

This card set contains limits for heat-transfer rate plots and is required only when IFLG7 = 1. There must be two cards for each plot page desired. The first card determines the limits on the axes of the graph. The second card defines the initial and final station numbers, as determined from the heating location input list, for which curves are to be plotted on the graph. A maximum of five stations per graph is allowed. Repeat cards 1 and 2 for each additional graph desired.

### Card 1 - Axes Limits for Graph

| Card Cols | Format | Fortran Symbol | Description | Units |
|---|---|---|---|---|
| 1-10 | F10.1 | XMIN | Minimum time; usually 0.0 | sec |
| 11-20 | F10.1 | XMAX | Maximum time | sec |
| 21-30 | F10.1 | YMIN | Minimum heat-transfer rate usually 0.0 | $Btu/ft^2$-sec |
| 31-40 | F10.1 | YMAX | Maximum heat-transfer rate | $Btu/ft^2$-sec |

### Card 2 - Station Numbers To Be Plotted on Graph

| Card Cols | Format | Fortran Symbol | Description |
|---|---|---|---|
| 1-5 | I5 | INIT | Initial station number on graph<br>NOTE: INIT ≤ IFINL |

Card 2 - (cont).

| Card Cols | Format | Fortran Symbol | Description |
|---|---|---|---|
| 6-10 | I5 | IFINL | Final station number on graph<br>NOTE: IFINL - INIT $\leq$ 4. For single curve per graph<br>INIT = IFINL |

## Punched Card Output

The punched-card output contains heating parameters at each station which can be used as input for the CMA and ASTHMA ablation and heat conduction programs. This option is used only when IFLG8 = 1.

| Card Cols | Format | Fortran Symbol | Description | Units |
|---|---|---|---|---|
| 1-2 | A2 | LST | -1, flag on last card for each heating location | |
| 3-10 | F8.3 | TIME | Time | sec |
| 11-20 | E10.4 | HR | Recovery enthalpy (JANAF) | Btu/lbm |
| 21-30 | BLANK | BLANK | Not used | |
| 31-40 | E10.4 | CH | Heat transfer coefficient | lbm/ft$^2$-sec |
| 41-50 | E10.4 | PE | Local boundary-layer edge pressure | atm |
| 51-60 | E10.4 | UE | Local boundary-layer edge velocity | ft-/sec |
| 61-70 | A10 | VCN | Identification marker from third title card | |
| 71 | BLANK | BLANK | Not used | |
| 72-79 | F8.3 | STN | Station location | in. |
| 80 | A1 | IFLG3 = L | Laminar heating | |
| | | = T | Turbulent heating | |
| | | = S | Stagnation - point heating (not currently used) | |

## Output

The first page of output from the program consists of heading information and a playback of data and options which were supplied to the program as input (Figure 6). The second page of output (Figure 7) lists the freestream conditions as input by the user. Subsequent pages of output list the computed boundary-layer edge conditions and heat transfer rates. Depending upon the option chosen, output is printed either at all times for each station location or at all stations for each time in the trajectory. Figure 8 shows output obtained using the first option. When punched cards are desired, a listing of the punched deck follows the boundary-layer edge conditions (Figure 9). Figure 10 is an example of the type of plot obtainable when requested by the user.

## Concluding Remarks

This report has presented the equations, operating procedure, and details of the LOVEL aerodynamic heating program. This program is currently operational on the CDC 7600 computer at SNLA. The control cards to execute the program are listed in Appendix D. Several modifications and improvements are being made to the program to make it more accurate. These subjects will be discussed in future reports on the LOVEL program. The program source deck is available from the author upon request.

```
                    LOW VELOCITY HEAT TRANSFER CODE
                              (LOVEL)

                        WRITTEN BY A. L. THORNTON
                              DIV 5633
                        SANDIA NATIONAL LABORATORIES
                          ALBUQUERQUE, NEW MEXICO

      COMPUTES THE B.L. EDGE CONDITIONS FOR SUBSONIC AND SUPERSONIC FLOW
      OVER A FLAT PLATE, WEDGE, OR SHARP CONE (0 .LE. MACH NO. .LE. 3).
   COLD-WALL HEAT TRANSFER CALCULATION USES REFERENCE TEMPERATURE TO COMPUTE FLUID
 PROPERTIES. PERFORMS CALCULATION OF LOCAL RECOVERY ENTHALPY AND STANTON NUMBER  FOR
     LAMINAR AND/OR TURBULENT FLOW AT DESIGNATED STATIONS (TRANSITION--OPTIONAL).

*****************************************************************************************************************
THORNTON 05-12-81  LOVEL
THE FOLLOWING RUN IS FOR VEHICLE "TEST"
"TEST"
*****************************************************************************************************************
THE FOLLOWING ANALYSIS IS FOR WEDGE FLOW AT ZERO ANGLE OF ATTACK WITH WEDGE HALF-ANGLE EQUAL TO 10.000 DEGREES.


HEAT TRANSFER CALCULATIONS WERE MADE AT THE FOLLOWING ARC LOCATIONS
                49.109
TRANSITION CRITERIA BASED ON AN ARC LENGTH REYNOLDS NUMBER
TRANSITION REYNOLDS NUMBER = .1000E+08
```

Figure 6. Heading Information and Summary of Input Variables

***FREESTREAM CONDITIONS***

| TIME (SEC) | VEL (FT/SEC) | TEMPERATURE (DEG R) | PRESSURE (ATM) | DENSITY (LBM/FT3) | VISCOSITY (LBM/FT-SEC) | ENTHALPY (BTU/LBM) | MACH |
|---|---|---|---|---|---|---|---|
| 0. | .300E+04 | .321E+03 | .130E-05 | .159E-06 | .811E-05 | .774E+02 | .341E+01 |
| .400E+01 | .250E+04 | .516E+03 | .762E+00 | .584E-01 | .120E-04 | .124E+03 | .224E+01 |
| .500E+01 | .316E+04 | .509E+03 | .701E+00 | .544E-01 | .119E-04 | .123E+03 | .285E+01 |
| .600E+01 | .386E+04 | .499E+03 | .631E+00 | .500E-01 | .117E-04 | .120E+03 | .352E+01 |
| .640E+01 | .411E+04 | .494E+03 | .601E+00 | .481E-01 | .116E-04 | .119E+03 | .377E+01 |
| .660E+01 | .411E+04 | .491E+03 | .586E+00 | .472E-01 | .116E-04 | .118E+03 | .377E+01 |
| .700E+01 | .405E+04 | .497E+03 | .562E+00 | .456E-01 | .115E-04 | .117E+03 | .374E+01 |
| .800E+01 | .392E+04 | .493E+03 | .537E+00 | .440E-01 | .114E-04 | .116E+03 | .363E+01 |
| .100E+02 | .378E+04 | .453E+03 | .383E+00 | .340E-01 | .108E-04 | .109E+03 | .362E+01 |
| .120E+02 | .368E+04 | .431E+03 | .303E+00 | .278E-01 | .104E-04 | .104E+03 | .361E+01 |
| .150E+02 | .361E+04 | .402E+03 | .216E+00 | .212E-01 | .983E-05 | .969E+02 | .366E+01 |
| .175E+02 | .362E+04 | .379E+03 | .162E+00 | .169E-01 | .936E-05 | .913E+02 | .378E+01 |
| .200E+02 | .363E+04 | .357E+03 | .121E+00 | .134E-01 | .890E-05 | .861E+02 | .391E+01 |
| .350E+02 | .415E+04 | .393E+03 | .299E-01 | .301E-02 | .964E-05 | .947E+02 | .427E+01 |
| .400E+02 | .441E+04 | .401E+03 | .219E-01 | .216E-02 | .981E-05 | .966E+02 | .448E+01 |
| .450E+02 | .471E+04 | .407E+03 | .173E-01 | .168E-02 | .993E-05 | .981E+02 | .475E+01 |
| .480E+02 | .489E+04 | .410E+03 | .157E-01 | .151E-02 | .998E-05 | .987E+02 | .492E+01 |
| .510E+02 | .500E+04 | .412E+03 | .146E-01 | .140E-02 | .100E-04 | .991E+02 | .502E+01 |
| .550E+02 | .498E+04 | .413E+03 | .139E-01 | .133E-02 | .100E-04 | .995E+02 | .499E+01 |
| .650E+02 | .492E+04 | .413E+03 | .140E-01 | .134E-02 | .100E-04 | .994E+02 | .493E+01 |
| .700E+02 | .489E+04 | .411E+03 | .150E-01 | .144E-02 | .100E-04 | .990E+02 | .491E+01 |
| .750E+02 | .485E+04 | .408E+03 | .165E-01 | .160E-02 | .995E-05 | .984E+02 | .489E+01 |
| .800E+02 | .467E+04 | .404E+03 | .197E-01 | .193E-02 | .986E-05 | .973E+02 | .473E+01 |
| .900E+02 | .449E+04 | .390E+03 | .341E-01 | .346E-02 | .957E-05 | .939E+02 | .463E+01 |
| .950E+02 | .407E+04 | .384E+03 | .419E-01 | .431E-02 | .945E-05 | .924E+02 | .423E+01 |
| .110E+03 | .359E+04 | .362E+03 | .687E-01 | .751E-02 | .899E-05 | .872E+02 | .384E+01 |
| .120E+03 | .317E+04 | .373E+03 | .149E+00 | .158E-01 | .922E-05 | .897E+02 | .334E+01 |
| .130E+03 | .259E+04 | .436E+03 | .321E+00 | .291E-01 | .105E-04 | .105E+03 | .252E+01 |
| .140E+03 | .189E+04 | .478E+03 | .512E+00 | .423E-01 | .113E-04 | .115E+03 | .176E+01 |
| .151E+03 | .144E+04 | .527E+03 | .860E+00 | .645E-01 | .122E-04 | .127E+03 | .128E+01 |

Figure 7. Freestream Conditions Used As Input

* * * * * * * * * * * * * * * * * * * * * * * *
RESULTS AT OTATION LOCATION = .4911E+02

| TIME (SECS) | UEDGE (FT/SEC) | TEDGE (DEG R) | PEDGE (ATM) | RHOEDGE (LBM/FT3) | MUEDGE (LBM/FT-SEC) | HE (BTU/LBM) (JANAF) | QDOT (BTU/FT2-SEC) | MACH | |
|---|---|---|---|---|---|---|---|---|---|
| 0.000 | .282E+04 | .410E+03 | .299E-05 | .278E-06 | .995E-05 | -.302E+02 | .168E-02 | .284E+01 | L |
| 4.000 | .226E+04 | .612E+03 | .135E+01 | .875E-01 | .136E-04 | .186E+02 | .236E+02 | .186E+01 | T |
| 5.000 | .293E+04 | .627E+03 | .140E+01 | .883E-01 | .139E-04 | .222E+02 | .418E+02 | .239E+01 | T |
| 6.000 | .363E+04 | .641E+03 | .143E+01 | .885E-01 | .141E-04 | .255E+02 | .650E+02 | .292E+01 | T |
| 6.400 | .388E+04 | .646E+03 | .144E+01 | .879E-01 | .142E-04 | .267E+02 | .741E+02 | .312E+01 | T |
| 6.600 | .388E+04 | .643E+03 | .140E+01 | .863E-01 | .141E-04 | .261E+02 | .724E+02 | .312E+01 | T |
| 7.000 | .382E+04 | .636E+03 | .134E+01 | .831E-01 | .140E-04 | .244E+02 | .673E+02 | .309E+01 | T |
| 8.000 | .370E+04 | .626E+03 | .125E+01 | .790E-01 | .139E-04 | .219E+02 | .594E+02 | .301E+01 | T |
| 10.000 | .356E+04 | .586E+03 | .902E+00 | .609E-01 | .132E-04 | .123E+02 | .408E+02 | .300E+01 | T |
| 12.000 | .347E+04 | .557E+03 | .701E+00 | .497E-01 | .127E-04 | .548E+01 | .306E+02 | .300E+01 | T |
| 15.000 | .340E+04 | .522E+03 | .506E+00 | .383E-01 | .121E-04 | -.299E+01 | .216E+02 | .304E+01 | T |
| 17.500 | .342E+04 | .496E+03 | .388E+00 | .309E-01 | .116E-04 | -.924E+01 | .171E+02 | .313E+01 | T |
| 20.000 | .343E+04 | .472E+03 | .299E+00 | .250E-01 | .112E-04 | -.151E+02 | .135E+02 | .322E+01 | T |
| 35.000 | .395E+04 | .532E+03 | .790E-01 | .587E-02 | .123E-04 | -.598E+00 | .782E+00 | .349E+01 | L |
| 40.000 | .420E+04 | .552E+03 | .602E-01 | .431E-02 | .126E-04 | .406E+01 | .797E+00 | .365E+01 | L |
| 45.000 | .449E+04 | .571E+03 | .501E-01 | .347E-02 | .129E-04 | .862E+01 | .856E+00 | .384E+01 | L |
| 48.000 | .467E+04 | .581E+03 | .463E-01 | .318E-02 | .131E-04 | .111E+02 | .905E+00 | .395E+01 | L |
| 51.000 | .479E+04 | .588E+03 | .444E-01 | .299E-02 | .132E-04 | .127E+02 | .933E+00 | .403E+01 | L |
| 55.000 | .476E+04 | .588E+03 | .420E-01 | .282E-02 | .132E-04 | .129E+02 | .897E+00 | .400E+01 | L |
| 65.000 | .470E+04 | .586E+03 | .417E-01 | .282E-02 | .132E-04 | .122E+02 | .869E+00 | .396E+01 | L |
| 70.000 | .467E+04 | .582E+03 | .446E-01 | .303E-02 | .131E-04 | .114E+02 | .885E+00 | .395E+01 | L |
| 75.000 | .463E+04 | .578E+03 | .493E-01 | .334E-02 | .131E-04 | .103E+02 | .907E+00 | .393E+01 | L |
| 80.000 | .446E+04 | .565E+03 | .563E-01 | .397E-02 | .128E-04 | .733E+01 | .892E+00 | .382E+01 | L |
| 90.000 | .428E+04 | .542E+03 | .965E-01 | .704E-02 | .124E-04 | .165E+01 | .104E+01 | .375E+01 | L |
| 95.000 | .386E+04 | .518E+03 | .110E+00 | .936E-02 | .120E-04 | -.404E+01 | .794E+01 | .346E+01 | T |
| 110.000 | .339E+04 | .476E+03 | .167E+00 | .139E-01 | .112E-04 | -.142E+02 | .820E+01 | .317E+01 | T |
| 120.000 | .297E+04 | .473E+03 | .325E+00 | .272E-01 | .112E-04 | -.149E+02 | .105E+02 | .279E+01 | T |
| 130.000 | .237E+04 | .525E+03 | .601E+00 | .452E-01 | .121E-04 | -.223E+01 | .113E+02 | .211E+01 | T |
| 140.000 | .163E+04 | .555E+03 | .847E+00 | .604E-01 | .127E-04 | .479E+01 | .671E+01 | .141E+01 | T |

WEDGE OR CONE ANGLE EXCEEDS THE MAXIMUM FOR GIVEN FREESTREAM MACH NUMBER OF 1.281 SHOCK IS DETACHED.

Figure 8. Computed Boundary-Layer Edge Conditions

PUNCHED CARD OUTPUT

| TIME | HR | CH | PE | UE | VCN | STN |
|---|---|---|---|---|---|---|
| 0.000 | .1024E+03 | .1641E-04 | .2882E-05 | .2916E+04 | "TEST" | 49.109L |
| 4.000 | .1088E+03 | .2167E+00 | .1354E+01 | .2257E+04 | "TEST" | 49.109T |
| 5.000 | .1739E+03 | .2406E+00 | .1393E+01 | .2931E+04 | "TEST" | 49.109T |
| 6.000 | .2573E+03 | .2526E+00 | .1435E+01 | .3626E+04 | "TEST" | 49.109T |
| 6.400 | .2925E+03 | .2533E+00 | .1437E+01 | .3885E+04 | "TEST" | 49.109T |
| 6.600 | .2912E+03 | .2485E+00 | .1404E+01 | .3880E+04 | "TEST" | 49.109T |
| 7.000 | .2920E+03 | .2387E+00 | .1336E+01 | .3824E+04 | "TEST" | 49.109T |
| 8.000 | .2627E+03 | .2260E+00 | .1251E+01 | .3696E+04 | "TEST" | 49.109T |
| 10.000 | .2360E+03 | .1729E+00 | .9023E+00 | .3560E+04 | "TEST" | 49.109T |
| 12.000 | .2180E+03 | .1406E+00 | .7012E+00 | .3469E+04 | "TEST" | 49.109T |
| 15.000 | .2014E+03 | .1075E+00 | .5057E+00 | .3401E+04 | "TEST" | 49.109T |
| 17.500 | .1973E+03 | .9649E-01 | .3883E+00 | .3417E+04 | "TEST" | 49.109T |
| 20.000 | .1933E+03 | .6963E-01 | .2986E+00 | .3432E+04 | "TEST" | 49.109T |
| 35.000 | .2566E+03 | .3048E-02 | .7900E-01 | .3945E+04 | "TEST" | 49.109L |
| 40.000 | .2948E+03 | .2705E-02 | .6021E-01 | .4137E+04 | "TEST" | 49.109L |
| 45.000 | .3411E+03 | .2509E-02 | .5015E-01 | .4492E+04 | "TEST" | 49.109L |
| 48.000 | .3704E+03 | .2444E-02 | .4679E-01 | .4670E+04 | "TEST" | 49.109L |
| 51.000 | .3902E+03 | .2392E-02 | .4440E-01 | .4797E+04 | "TEST" | 49.109L |
| 55.000 | .3862E+03 | .2324E-02 | .4195E-01 | .4761E+04 | "TEST" | 49.109L |
| 65.000 | .3759E+03 | .2312E-02 | .4175E-01 | .4698E+04 | "TEST" | 49.109L |
| 70.000 | .3707E+03 | .2388E-02 | .4465E-01 | .4670E+04 | "TEST" | 49.109L |
| 75.000 | .3640E+03 | .2493E-02 | .4887E-01 | .4632E+04 | "TEST" | 49.109L |
| 80.000 | .3343E+03 | .2665E-02 | .5682E-01 | .4457E+04 | "TEST" | 49.109L |
| 90.000 | .3036E+03 | .3436E-02 | .9649E-01 | .4278E+04 | "TEST" | 49.109L |
| 95.000 | .2591E+03 | .3066E-01 | .1096E+00 | .3861E+04 | "TEST" | 49.109T |
| 110.000 | .1895E+03 | .4325E-01 | .1663E+00 | .3393E+04 | "TEST" | 49.109T |
| 120.000 | .1415E+03 | .7405E-01 | .3258E+00 | .2971E+04 | "TEST" | 49.109T |
| 130.000 | .9752E+02 | .1154E+00 | .6087E+00 | .2371E+04 | "TEST" | 49.109T |
| 140.000 | .5185E+02 | .1295E+00 | .8475E+00 | .1628E+04 | "TEST" | 49.109T |

WEDGE OR CONE ANGLE EXCEEDS THE MAXIMUM FOR GIVEN FREESTREAM MACH NUMBER OF 1.281 SHOCK IS DETACHED.

**Figure 9.** Listing of Punched Card Output

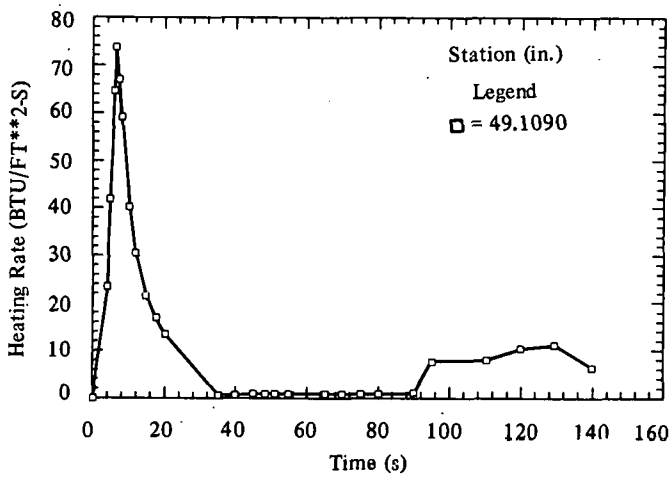


**Figure 10.** Sample Plot Obtained From Program LOVEL

# APPENDIX A

## Minimum Freestream Mach Number for Attached Shock as a Function of Semivertex Angle

If the freestream Mach number goes below the corresponding minimum Mach number ($M_{min}$) for the wedge or cone angles listed in Tables A-1 and A-2, respectively, the shock becomes detached and the governing equations for supersonic flow are no longer applicable.

**Table A-1. Minimum Mach Number as a Function of Wedge Semivertex Angle**

| δ (deg) | Mmin |
|---|---|
| 0.56 | 1.05 |
| 1.52 | 1.10 |
| 2.67 | 1.15 |
| 3.94 | 1.20 |
| 5.29 | 1.25 |
| 6.66 | 1.30 |
| 8.05 | 1.35 |
| 9.43 | 1.40 |
| 10.79 | 1.45 |
| 12.11 | 1.50 |
| 13.40 | 1.55 |
| 14.65 | 1.60 |
| 15.86 | 1.65 |
| 17.01 | 1.70 |

**Table A-2. Minimum Mach Number as a Function of Cone Semivertex Angle[8]**

| δ (deg) | Mmin |
|---|---|
| 5.0 | 1.0129 |
| 7.5 | 1.0294 |
| 10.0 | 1.0528 |
| 12.5 | 1.0828 |
| 15.0 | 1.1193 |
| 17.5 | 1.1622 |

Tables A-2 and A-3 are shown in graphical form in Figure A-1.

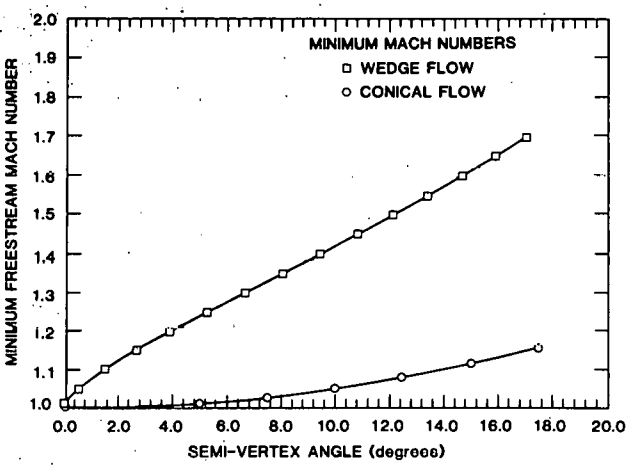


**Figure A-1.** Minimum Freestream Mach Number for Attached Shock as a Function of Semivertex Angle

# APPENDIX B

## Boundary-Layer Transition or Relaminarization

One of the most critical elements in estimating the heat-transfer coefficient over a body is in determining whether the flow about the body is laminar or turbulent. Papers written on this subject agree that a transition-relaminarization criterion is dependent upon many parameters (surface roughness, freestream disturbances, external pressure gradient, etc). For the particular problem of aerodynamic heating at low velocities, it is more conservative — in the case of temperature predictions — to have relaminarization occurring at higher local Reynolds numbers since convective cooling is less for the laminar boundary layer. Reference 9 suggests that on a flat-plate, transition takes place at a distance S from the leading edge when the local Reynolds number is

$$Re_x = \frac{\rho_e U_e S}{\mu_e} = 3.5 \times 10^5 \text{ to } 10^6 .$$

Reference 3 gives a range of local Reynolds number for transition of

$$Re_x = 3.0 \times 10^5 \text{ to } 5.0 \times 10^7 .$$

Other means have been suggested for determining the point of transition-relaminarization. The authors of Reference 3 suggest that a Reynolds number based on the momentum thickness, $\Delta$, is a better criterion for determining the critical point of transition. When integrated along the surface, the value of $\Delta$ is appropriately influenced by freestream disturbances, pressure gradients, or mass transfer at the surface. For the purpose of this analysis, it was decided that a Reynolds number based on the arc location with a value of

$$Re_s = 1.0 \times 10^6$$

is satisfactory for determining transition. If the flow is initially turbulent, as in the case of a sounding rocket exiting the atmosphere, a relaminarization Reynolds number of

$$Re_s = 1.0 \times 10^7$$

is used instead.

# APPENDIX C

## Newton-Raphson Method

Given a function, $f(x) = 0$, it is the user's desire to find the value of x which satisfies the equation. Use of the Newton-Raphson (N-R) method allows one to solve for the correct value of x, using a very simple and systematic approach. Essentially, the method involves little more than a local linearization of the function about some initial guess for the root of the function; call it $x_o$. In the neighborhood of $x_o$, one can approximate the function by the first two terms in the Taylor series expansion:

$$f(x) = f(x_o) + (x - x_o)\, f'(x_o) \quad . \tag{C-1}$$

This is equivalent to approximating the function by the tangent line. The next approximation to the root (call it $x_1$) is taken to be the root of the linear approximation Eq (C-1), so that

$$x_1 = x_o - \frac{f(x_o)}{f'(x_o)} \quad . \tag{C-2}$$

Having this improved estimate, one can simply repeat the procedure using the formula:

$$x_{j+1} = x_j - \frac{f(x_j)}{f'(x_j)} \tag{C-3}$$

until $|x_{j+1} - x_j| \leq \epsilon$, where $\epsilon \leq 10^{-3}$.

In order for the N-R method to work properly, a good initial guess for $x_o$ is imperative. Hence, to determine the shock angle, $\theta_s$, define from Eq (31),

$$f(\theta_s) = C_1 - \tan(\theta_s)\left\{\frac{C_2}{\beta^2 - 1} - 1\right\} = 0 \tag{C-4}$$

where

$$C_1 = \cot \delta_{wg}$$

$$C_2 = \frac{\gamma + 1}{2} M_\infty^2 = \frac{6}{5} M_\infty^2$$

$$\beta = M_\infty \sin\theta \quad .$$

Multiplying Eq (C-4) by $(\beta^2 - 1)$ and differentiating, one obtains

$$f'(\theta_s) = (C_1 + \tan\theta_s)\, M_\infty^2 \sin 2\theta_s + (\beta^2 - 1 - C_2)\, \sec^2\theta_s \quad . \tag{C-5}$$

To obtain an initial estimate for the shock angle, the following relations were used

$$\theta\omega_s = \begin{cases} 90 - 60(M_\infty - 1) + \delta_{wg} & \text{for } 1 \leq M_\infty \leq 2 \\ 30 - 10.53(M_\infty - 2) + 0.75\,\delta_{wg} & \text{for } 2 \leq M_\infty < 3 \quad . \end{cases} \tag{C-6}$$

Using Eq (C-3), the iterative process can continue until the desired convergence is obtained.

# APPENDIX D

## System Control Cards

In order to have the LOVEL Program accepted on the secure NOS/Scope 2.1 operating systems at SNLA, the following control cards are necessary:

```
JOB,ST---,T50.
USER(USERNUM,PASSWRD)
CHARGE(ACCOUNT)
PFGET(LGO,LOVELL,CL=UNCL,AU=ALTHORN)
COPYCR,INPUT,TAPE5.
REWIND,TAPE5.
COPYSBF,TAPE5,OUTPUT.
REWIND,TAPE5.
PFGET(DISS,AU=PLOTLIB)
BEGIN,DISS,DISS,HC1,E=NOGO,F=F4.
DISSABS,PL=50000.
PFGET(RHCNBPC,AU=PLOTLIB)
BEGIN,RHC,RHCNBPC,TAPE77.
COMQ,TAPE76,HC1,CS=XX.
  (where XX=RJET SITE, e.g., CS=R7)
.
.
.
E-O-R
```

To use the source code and to obtain a listing of the program, one should use the following control cards:

```
JOB,ST---,T50.
USER(USERNUM,PASSWRD)
CHARGE(ACCOUNT)
PFGET(OLDPL,LOVELS,CL=UNCL,AU=ALTHORN)
UPDATE(F,W,C=SOURCE)
COPYCR,INPUT,TAPE5.
REWIND,TAPE5.
COPYSBF,TAPE5,OUTPUT.
REWIND,TAPE5.
FTN,I=SOURCE,R=2.
PFGET(DISS,AU=PLOTLIB)
BEGIN,DISS,DISS,HC1,E=NOGO,F=F4.
DISSABS,PL=50000.
PFGET(RHCNBPC,AU=PLOTLIB)
BEGIN,RHC,RHCNBPC,TAPE77.
COMQ,TAPE76,HC1,CS=XX.
.
.
.
E-O-R
E-O-R
```

# References

[1]Frank M. White, *Viscous Fluid Flow* (New York: McGraw-Hill, 1974).

[2]H. Evans, *Laminar Boundary-Layer Theory* (New York: McGraw-Hill, 1968).

[3]W. M. Kays, M. E. Crawford, *Convective Heat and Mass Transfer*, (2nd ed, New York: McGraw-Hill, 1980).

[4]R. E. Wilson, *Handbook of Supersonic Aerodynamics*, Sections 13 and 14, "Viscosity and Heat Transfer Effects," NAVORD Report 1488. (White Oak, MD: US Naval Ordnance Laboratory, August 1966), Vol 5.

[5]N. F. Krasnov, *Aerodynamics of Bodies of Revolution* (New York: American Elsevier Publishing Co., Inc, 1970).

[6]Ames Research Staff, *Equations, Tables and Charts for Compressible Flow*, NACA Report 1135, (Moffett Field, CA: Ames Aeronautical Laboratory, 1953).

[7]G. J. Hochrein, *A Procedure for Computing Aerodynamic Heating on Sphere Cones - Program BLUNTY, Volume II: Equations, Operating Procedure, and Program Details*, SC-DR-69-449 (Albuquerque, NM: Sandia Laboratories, November 1969).

[8]Massachusetts Institute of Technology Staff of the Computing Section Center of Analysis, *Tables of Supersonic Flow Around Cones*, Technical Report No. 1 (Cambridge, MA: 1947).

[9]H. Schlichting, *Boundary-Layer Theory* (7th ed, New York: McGraw-Hill, 1979).

## Distribution:

NASA Goddard Space Flight Center (2)
Sounding Rocket Division
Flight Performance Branch
Greenbelt, MD 20771
Attn: L. D. Wing
J. Lane

NASA Wallops Flight Center
SRPB/PAS
Bldg. E-108
Wallops Island, VA 23337
Attn: W. Gurkin

Thiokol Corp. (2)
Astronet Division
3340 Airport Road
Odgen, UT 84402
Attn: G. Alford
R. G. Moore

General Dynamics Corporation (2)
Pamona Division
P. O. Box 2507
Pamona, CA 91766
Attn: D. Andersen
D. Roberts

NASA Ames Research Center
Entry Technology Branch
Moffet Field, CA 91035
Attn: H. Figuerda 234-1

Martin Marietta Aerospace
Denver Division
P. O. Box 179
Denver, CO 80201
Attn: L. J. Rogers S-8018

Naval Surface Weapons Center
White Oak
Silver Springs, MD 20910
Attn: E. W. DeKnight,
Code G40

400 C. W. Winter
5000 J. K. Galt
5600 D. B. Shuster
Attn: R. C. Maydew, 5630
5610 A. A. Lieber
5620 M. M. Newsom
5631 H. R. Vaughn
5632 C. W. Peterson
5633 S. McAlees
5633 L. W. Connell
5633 S. G. Beard
5633 M. L. Carnicom
5633 A. L. Thornton (6)
5634 D. D. McBride
5635 W. R. Barton
5636 J. K. Cole (2)
Attn: D. E. Larson
R. Palmer
5650 D. J. Rigali
Attn: M. W. Sterk, 5651
A. C. Bustamante, 5652
E. C. Rightley, 5653
J. J. Bahlman, 5653
E. . Steinkraus, 5653
8110 J. Barham
Attn: J. D. Gilson, 8112
8214 M. A. Pound
3141 L. J. Erickson (5)
3151 W. L. Garner (3)
3154 C. H. Dalin (25)
For DOE/TIC (Unlimited Release)

| Org. | Bldg. | Name | Rec'd by | Org. | Bldg. | Name | Rec'd by |
|---|---|---|---|---|---|---|---|
| | | | | | | | |
| | | | | | | | |
| | | | | | | | |
| | | | | | | | |
| | | | | | | | |
| | | | | | | | |
| | | | | | | | |
| | | | | | | | |
| | | | | | | | |
| | | | | | | | |
| | | | | | | | |
| | | | | | | | |
| | | | | | | | |
| | | | | | | | |
| | | | | | | | |

Sandia National Laboratories